Available online at www.sciencedirect.com
SCIENCE DIRECT
Journal of Power Sources 152 (2005) 22–26
JOURNAL OF POWER SOURCES
www.elsevier.com/locate/jpowsour

Electrochemical characterization and performance evaluation of intermediate temperature solid oxide fuel cell with $La_{0.75}Sr_{0.25}CuO_{2.5-\delta}$ cathode

Ho-Chieh Yu [a,*], Feng Zhao [b], Anil V. Virkar [b], Kuan-Zong Fung [a]

[a] *Department of Material Science and Engineering, National Cheng Kung University, No. 1, University Road, Tainan 70101, Taiwan, ROC*
[b] *Department of Material Science and Engineering, University of Utah, Salt Lake City, UT 84112, USA*

Received 26 February 2005; received in revised form 8 March 2005; accepted 8 March 2005
Available online 8 June 2005

Abstract

This study presents the woks on the electrochemical characterization and performance evaluation of using $La_{0.75}Sr_{0.25}CuO_{2.5-\delta}$ (LSCu) as cathode material for intermediate temperature solid oxide fuel cell (IT-SOFC). The cell performance measurement was conducted on the Ni–YSZ anode supported single cell using the yittria-stabilized zirconia (YSZ) thin film (ca. 8 μm) as electrolyte, and porous LSCu layer as cathode (ca. 80 μm). The AC-impedance analyses were carried out by electrolyte supported LSCu/YSZ/Pt half-cell because of the thin YSZ film and the unsymmetrical between cathode and anode in the anode supported single cell may lose the accuracy. According to the analyses of the AC-impedance spectra, the spectra can be characterized by two arcs. The larger arc at low frequencies maybe attributed to the electrode polarization caused by the adsorption/desorption of the molecular oxygen, and the diffusion of oxygen ions. On the other hand, the much smaller one at high frequencies was attributed to the polarization during charge-transfer. The interface resistance was decreased by current passing. After 30 min of 200 mA cm^{-2} current was passed, the overall resistance was decreased from 5.01 to 0.25 Ω. For the performance testing, the maximum power density at 800 °C is 0.65 W cm^{-2} with 150 and 500 sccm of hydrogen and air flows, respectively. According to these results, LSCu is a potential cathode material for the IT-SOFC.

Keywords: Intermediate-temperature solid oxide fuel cell; LSCu; AC-impedance; Perovskite oxide; Cathode material; Performance

1. Introduction

Solid oxide fuel cell has emerged as one of the most important power generation technologies because of its high-energy conversion efficiency, low noise, and low pollution. With the development of thin film technique of electrolyte layer for the SOFC, the operating temperature can be reduced to 600–800 °C [1–6]. When SOFC operates at such a lower temperature, it provides long-term cell material stability, and minimize the material corrosion for plant component. Nevertheless, both the ohmic loss of the electrolyte and the polarization loss of the electrodes are increased. To reduce the polarization resistance between electrode/electrolyte is important for the development of IT-SOFC. It is well known that the mostly common used cathode material, (La, Sr)MnO_3 (LSM) is a poor oxygen ion conductor [7,8]. Consequently, the overpotential loss for the O_2 reduction reaction on the cathode/electrolyte interface is relatively high in thin film SOFC [9–11]. Hence, seeking for a cathode material with higher oxygen ion conductivity and the reaction activity for O_2 reduction is believed to be a good way to enhance the performance of IT-SOFC.

Recently, the oxygen-deficient perovskite oxide, $La_{1-x}Sr_xCuO_{2.5-\delta}$, have been investigated as a potential cathode mate-

* Corresponding author. Tel.: +886 6 2380208; fax: +886 6 2380208.
E-mail addresses: kzfung@mail.ncku.edu.tw, close@mse.ncku.edu.tw (H.-C. Yu).

0378-7753/$ – see front matter © 2005 Elsevier B.V. All rights reserved.
doi:10.1016/j.jpowsour.2005.03.173

rial for IT-SOFC [12]. This material provides an appropriate electrical conductivity of about 800 S cm^{-1} at 800 °C, a large amount of oxygen vacancies (more than 16.7%), and a good electrochemical activity toward the molecular oxygen reduction [13]. In this study, performance of anode supported single cell using LSCu as cathode material was evaluated, also the electrochemical behavior at the cathode/electrolyte was investigated by AC-impedance analyses.

2. Experimental

2.1. LSCu powder and paste preparation

Strontium doped lanthanum copper oxide, $La_{0.75}Sr_{0.25}CuO_{2.5-\delta}$, powder was prepared by conventional ceramic processing. An appropriate ratio of La_2O_3, $SrCO_3$, and CuO powders were adequately mixed by ball-milling in ethanol solution for 24 h. After the powder mixture was calcined at 950 °C for 24 h in air, it was ball-milled again for 120 h to make fine powder. The LSCu paste was made form ball-milled LSCu powder and an appropriate amount of ethylene glycol (EG).

2.2. Electrochemical testing

The electrochemical testing in this study was carried out by AC-impedance spectroscopy using three electrode methode (working, counter and reference electrode). Due to the anode supported cell may cause the accuracy losing because of the current effect on the reference electrode, therefore, the testing samples were prepared in electrolyte supported LSC/YSZ/Pt half-cell. The 8% yittria-stabilized zirconia (8YSZ) dense disk of 19 mm in dia. and 0.5 mm in thickness was used as electrolyte. The LSCu paste was applied on the one side of the electrolyte by screen-printing method. Platinum paste was applied on the other side as the counter electrode, and on the edge of the cathode side as the reference electrode. The geometrical area of both working (LSCu) and counter (Pt) electrodes was 64 mm^2 (9.0 mm in dia.), and the distance between working electrode and reference electrode is about 10 mm, which was about 17 times longer than the electrolyte thickness. Then the samples were heated at 850 °C for 5 h.

2.3. Single cell fabrication and testing

The Ni/YSZ anode support was prepared by the powder mixture of 30 wt.% of 8YSZ (Tosoh) and 70 wt.% of NiO (Alfa). After adequately mixed, the powder mixture was compacted under uniaxial pressure to form a disc. And then the compacted discs were heated at 950 °C for 2 h, the sturdier green anode discs were created. On the other hand, the slurries of 50 wt.% of NiO/50 wt.% YSZ (NiO/YSZ), and YSZ in ethanol were prepared for anode/electrolyte interlayer and electrolyte layer fabrication, respectively. After appropriate amount of the NiO/YSZ and YSZ slurries were applied on one side of the green anode, the specimens were sintered at 1400 °C for 2 h in air. Then the LSCu paste was applied onto the YSZ electrolyte layer in an area of 1 cm^2. Finally, the specimens were heated at 900 °C for 2 h in air.

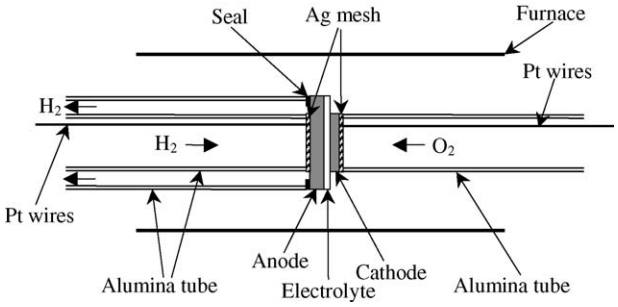

Fig. 1. Illustration of the experimental cell testing arrangement.

As illustrated in Fig. 1 the single cell testing stand consists of two alumina tubes in between where a cell can be secured. On both electrode sides, the Ag meshes were used as current collectors. The fixed hydrogen flow (150 sccm), and air flow (500 sccm) were supplied into the anode and cathode side of the cell, respectively, via alumina tubes. The cell was heated at the furnace gradually to 800 °C for 5 h to reduce the NiO of the anode support to Ni, and then the cell performance was tested between 650 and 800 °C.

3. Results and discussion

3.1. Impedance analyses

Perovskite strontium doped lanthanum cuprate has been investigated as a potential cathode material for a IT-SOFC. In this study, the LSCu/YSZ interface behavior of using $La_{0.75}Sr_{0.25}CuO_{2.5-\delta}$ as cathode material for IT-SOFC was investigated by AC-impedance examines. Fig. 2 shows the specific impedance spectra of the $La_{0.75}Sr_{0.25}CuO_{2.5-\delta}$/YSZ interface taken at 700 and 800 °C. The examinations were carried out at open-circuit voltage (OCV) in air before and after passing a 200 mA cm^{-2} of current for 3 and 30 min. The spectra can be characterized by a larger arc at low frequencies and a much smaller one at high frequencies. These results indicate that there are at least two electrode processes corresponding to the high and low frequency arcs during molecular oxygen reduction. According to Heuveln and Bouwmeester [9] and Leng et al.'s works [14], the inductive high-frequency arc can be attributed to the polarization during charge transfer. On the other hand, the inductive low-frequency arc can be attributed to the oxygen adsorption and desorption on the electrode surface and the diffusion of the oxygen ions. Therefore, the impedance spectra were fitted to an equivalent circuit consisting of two parallel branches (R_{ct}, C_{dl}) and (R_d, CPE), as show in Fig. 3. The resistance R_b is denoted as the overall ohmics resistance including of

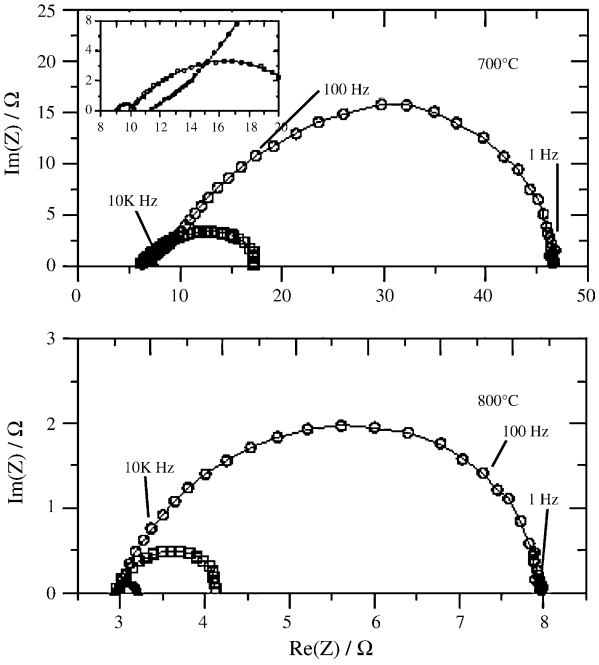

Fig. 2. Impedance spectra (at zero polarization) of $La_{0.7}Sr_{0.3}CuO_{2.5-\delta}$ before (◯) and 3 min (□) and 30 min (△) after passing a current of 200 mA cm^{-2}, and the measurements were taken at 700 and 800 °C, respectively.

ohmic electrolyte and electrode resistance the contact resistance at the electrode/electrolyte interface and between electrode and current collector. The resistance R_{ct} is interpreted as the charge-transfer resistance, and the capacitance C_{dl} as the double-layer capacitance, which is contributed by the surface contact of the electrode particles on the electrolyte surface. The R_d and CPE branch may relate to the oxygen adsorption/desorption on the electrode particle surface and the oxygen ions diffusion in the electrode [9].

The overall resistance of the sample significantly decreased when current being passed as shown in Fig. 2. For example, the overall resistance of the sample operating at 800 °C was 5.01 Ω. However, when the current of 200 mA cm^{-2} was passed 3 and 30 min, the overall resistance was decreased to 1.12 and 0.25 Ω, respectively. It was found that the size decreasing of the arc on the low frequencies (R_d-CPE) was relatively larger than that on the high frequencies. These results elucidate that the current pass greatly enhanced the oxygen adsorption/desorption on the electrode surface

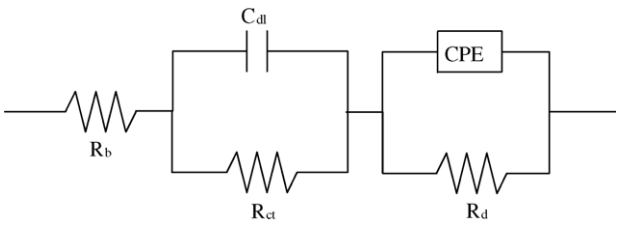

Fig. 3. Equivalent circuit model: R is resistance, C is capacitance, and CPE is a constant phase element.

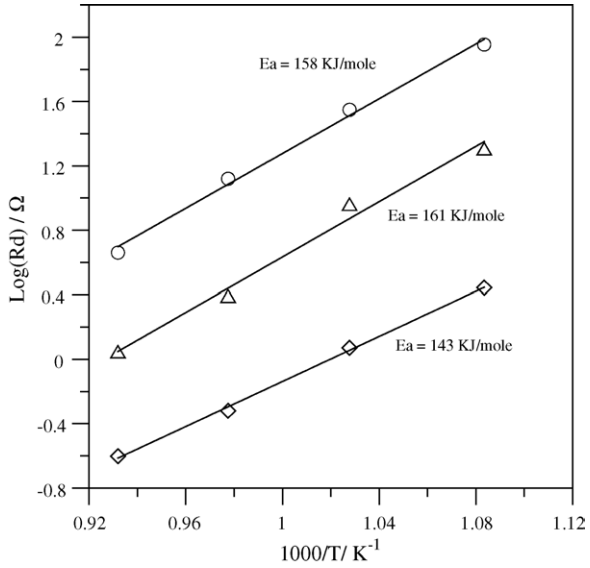

Fig. 4. The R_d value before (◯), and 3 min (△) and 3 h (◊) after passing a 200 mA cm^{-2} current as a function of inverse absolute temperature.

and the diffusion of the oxygen ions. Fig. 4 shows the log(R_d) value as a function of inverse absolute temperature before, and 3 and 30 min after passing a 200 mA cm^{-2} current. The R_d values decrease with increasing current passing time and the log(R_d) values decrease linearly with inverse absolute temperature increasing. However, the activation energies of the resistance R_d are between 143 and 161 kJ $mole^{-1}$. As mention above, the R_d is attributed by the oxygen adsorption and desorption and the diffusion of the oxygen ions. And it is known that the oxygen vacancies on the electrode surface provide the reaction site for the reduction of the molecular oxygen and the oxygen vacancies provide the pass way for the diffusion of reduced oxygen ions [15–17]. Therefore, the oxygen vacancies concentration of the cathode material should play an important role on the change of the R_d value. It has been investigated that the $La_{0.75}Sr_{0.25}CuO_{2.5-\delta}$ exhibit 16.67% of ordered oxygen vacancies and a small amount of disordered ones [18–20]. When the current was passed, the reduction of the molecular oxygen to oxygen ions on the triple phase boundary (TPB) can be greatly enhanced [21], and the oxygen-ion concentration gradient around the TPB region is then being increased [22]. Therefore, the diffusivity of the oxygen ions can be improved. This ionic conductivity improvement enhances the diffusion of the oxygen ions, which were reduced on the electrode surface from the electrode surface to the TPB. This phenomenon can be seen as the extending of the TPB. Also, the TPB can be extended by increasing the operating temperature. Therefore, the decreasing of R_d with increasing current passing time and operating temperature can be expected.

3.2. Performance evaluation

The cell performance evaluation in this study was carried out by anode supported single cell with YSZ thin film elec-

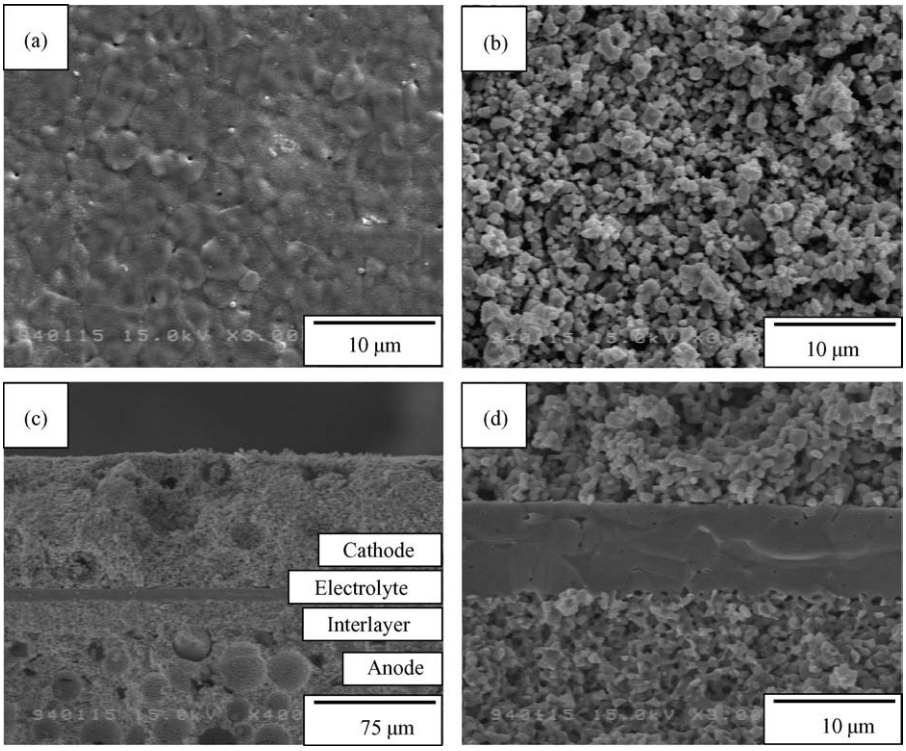

Fig. 5. The SEM microstructure of the anode support single cell: (a) top-view of the YSZ electrolyte layer, (b) top-view of the cathode layer, and (c), (d) cross-section of the cell.

trolyte and LSCu cathode. Fig. 5 shows the SEM micrographs of anode supported single cell applied with LSCu cathode layer. The top-view of the YSZ electrolyte layer and cathode layer are shown in Fig. 5(a) and (b), respectively. The cross-section of the anode supported single cell around the YSZ electrolyte were shown in Fig. 5(c) and (d) with different magnification. From Fig. 5(a) and (d), an 8 μm in thickness of dense YSZ thin film with a small amount of close pores was well adhered on the Ni/YSZ anode support. Fig. 5(c) and (d) show the cross-section of the single cell, an about 20 μm thick of electrolyte/anode interlayer is applied on the anode support, and an about 80 μm thick of cathode layer is applied on the electrolyte layer. As shown in Fig. 5(b) and (d), the anode, electrolyte/anode interlayer and cathode layer are fabricated in high porosity structures and the particles in these layers were well-necked. The particle sizes of the LSCu particles are in the size range of 0.5–1.5 μm.

Fig. 6 shows the variation of cell voltage and power density as a function of current density for the LSCu/YSZ/Ni–YSZ single cell operating at 700, 750 and 800 °C under 150 and 500 sccm of hydrogen and air flow, respectively. The OCV of the samples is about 1.12 V which is slightly higher than the theoretical value of 1.105 (as the anode side is fed with H_2 + 3 vol.% H_2O, and the cathode side is fed with air). This can be suspected that the H_2 was not saturated with water at time the experiment was conducted [14]. The area-specific resistance (ASR) of the cell calculating from the voltage vs. current curve are 0.32, 0.75, and 1.21 Ω cm^2 at 800, 750, and 700 °C, respectively. The ASR of the cell is mainly governed by both the ohmic resistance of YSZ and the polarization of the electrode due to the oxygen ion transfer and charge transfer on the electrode surface. In this anode supported single cell, the YSZ electrolyte layer was made in an about 8 μm thin film. Base on the YSZ ionic conductivity of about 0.04 S cm^{-1} at 800 °C [23], the ohmic resistance of 8 μm thick YSZ electrolyte is estimated to be 0.02 Ω cm^2. Therefore, the resistance cause by the YSZ ohmic resistance is

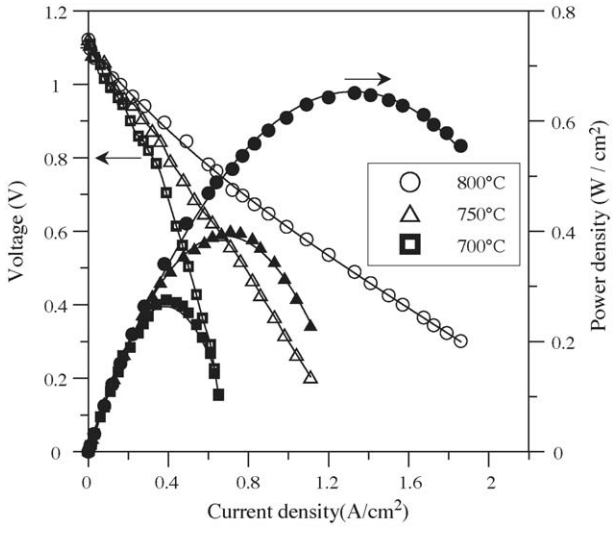

Fig. 6. The cell voltage and power density as a function of current density of the anode support single cell with $La_{0.75}Sr_{0.25}CuO_{2.5-\delta}$ cathode operating at 700, 750 and 800 °C.

relative small. On the other hand, the calculated ASR values are in good agreement with the polarization resistance analyses of the YSZ supported half cell by ac-impedance spectroscopy after passing a 200 mA cm^{-2} of current for 30 min as shown in Fig. 4. This indicates that the interface resistance of the single cell is mainly contributed by the polarization of the electrode. For a fuel cell application, the ASR of this cell operating at 750, and 700 °C is too high to provide effective power density. It is believed that microstructure optimization can lead to significant reductions in ASR especially when SOFC operating at a lower temperature.

Due to the increase of the ohmic resistance of the YSZ electrolyte and the polarization resistance on the electrode/electrolyte interface, the performance of the single cell is decreased with decreasing operating temperature. As shown in Fig. 6, the maximum cell power density is decreasing from 0.65 to 0.40, and 0.28 W cm^{-2} when the operating temperature is decreased from 800 to 750, and 700 °C, respectively. Since the polarization resistance at the cathode/electrolyte interface is the main reason affecting the single cell performance. Further LSCu compositional modification and microstructure optimization of the LSCu cathode layer will improve the performance of the cell. Therefore, the cathode particle size reduction or the oxygen ions pathway increasing by electrolyte material addition in cathode layer should yield significantly higher power densities.

4. Conclusion

In this study, the electrochemical characterization and performance evaluation of IT-SOFC using $La_{0.75}Sr_{0.25}CuO_{2.5-\delta}$ as cathode material were investigated. The polarization resistance of electrode/electrolyte interface measured by electrolyte supported sample was contributed by the charge-transfer, the adsorption/desorption on the electrode surface and the diffusion of the oxygen ions. For the performance testing carried out by anode supported single cell, the maximum cell power densities obtained are 0.65, 0.40, and 0.28 W cm^{-2} at 800, 750, and 700 °C, respectively. The ASR of the cell are 0.32, 0.75, and 1.21 Ω cm^2 at 800, 750, and 700 °C, respectively. These values are good agreement with the polarization resistance analyzed by AC-impedance spectroscopy after passing a 200 mA cm^{-2} of current for 30 min. Therefore, the main inter-resistance of the single cell may be contributed by the polarization at the cathode/electrolyte interface. For the further performance improvement, the LSCu compositional modification and microstructure optimization of the LSCu cathode layer will be adopted.

Acknowledgement

This work is financially support by the National Science Council of Taiwan, ROC (grant no. NSC 93-2120-M-006-004).

References

[1] T. Setoguchi, M. Sawano, K. Eguchi, H. Arai, Solid State Ionics 40–41 (1990) 502.
[2] J. Schoonman, J.P. Dekker, J.W. Broers, N.J. Kiwiet, Solid State Ionics 46 (1991) 299.
[3] V.E.J. van Dieten, J. Schoonman, Solid State Ionics 57 (1992) 141.
[4] C.C. Chen, M.M. Nasrallah, H.U. Anderson, Solid State Ionics 70–71 (1994) 101.
[5] T. Hibino, A. Hashimoto, K. Asano, M. Yano, M. Suzuki, M. Sano, Electrochem. Solid-State Lett. 5 (2002) A242.
[6] Z. Shao, S.M. Haile, Nature 431 (2004) 170.
[7] T. Horita, K. Yamaji, M. Ishikawa, N. Sakai, H. Yokokawa, T. Kawada, T. Kato, J. Electrochem. Soc. 145 (1998) 3196.
[8] J. Mizusaki, Y. Yonemura, H. Kamata, K. Ohyama, N. Mori, H. Takai, H. Tagawa, M. Dokiya, K. Naraya, T. Sasamoto, H. Inaba, T. Hashimpto, Solid State Ionics 132 (2000) 167.
[9] F.H. van Heuveln, H.J.M. Bouwmeester, J. Electrochem. Soc. 144 (1997) 134.
[10] B.C.H. Steele, Solid State Ionics 134 (2000) 3.
[11] S.P. Jiang, J. Power Sources 124 (2003) 390.
[12] H.C. Yu, K.Z. Fung, Mater. Res. Bull. 38 (2003) 231.
[13] H.C. Yu, K.Z. Fung, J. Power Sources 133 (2004) 162.
[14] Y.J. Leng, S.H. Chan, K.A. Khor, S.P. Jiang, Int. J. Hydrogen Energy 29 (2004) 1025.
[15] T. Ishihara, T. Kudo, H. Matsuda, Y. Takita, J. Electrochem. Soc. 142 (1995) 1519.
[16] S. Kim, S. Wang, X. Chen, Y.L. Yang, N. Wu, A. Ignatiev, A.J. Jacobson, B. Abeles, J. Electrochem. Soc. 147 (2000) 2398.
[17] T. Horita, K. Yamaji, N. Sakai, H. Yokokawa, T. Kawada, T. Kato, Solid State Ionics 127 (2000) 55.
[18] H. Yamaguchi, H. Mstsuhata, T. Ito, K. Oka, Physica C 282–287 (1997) 1079.
[19] B. Normand, D.F. Agterberg, T.M. Rice, Physica C 317–318 (1999) 511.
[20] H.C. Yu, K.Z. Fung, J. Mater. Res. 19 (2004) 943.
[21] T. Horita, K. Yamaji, N. Sakai, H. Yokokawa, A. Weber, E. Iver-Tiffee, J. Electrochem. Soc. 148 (2001) A456.
[22] S.P. Jiang, J.G. Love, J.P. Zhang, M. Hoang, Y. Ramprakash, A.E. Hughes, S.P.S. Badwal, Solid State Ionics 121 (1999) 1.
[23] N.M. Sammes, Z. Cai, Solid State Ionics 100 (1997) 39.